

Effects of Immersed Surfaces on the Combustor Efficiency of Small-Scale Fluidized Beds

Afsin GUNGOR*, Nurdil ESKIN
Istanbul Technical University, Mechanical Engineering Faculty,
34439 Gümüşsuyu, Istanbul, Turkey
Tel: +90 (505) 504 49 02; Fax: +90 (212) 245 07 95
E-mail: afsingungor@yahoo.com

Abstract

In this study, effects of the different types of heat exchanger surfaces on the second law efficiency of a small-scale circulating fluidized bed (CFB) combustor are analyzed and the results are compared with the bubbling fluidized bed coal combustor effectiveness values. Using a previously developed simulation program, combustor efficiency and entropy generation values are obtained at different operation velocities at different height and volume ratios of the immersed surfaces, both for circulating and bubbling fluidized bed combustors. Besides that, the influence of the immersed surface types on the combustor efficiency was compared for different fluidized bed combustors. Through this analysis, the dimensions, arrangement and type of the immersed surfaces which achieve maximum efficiency are obtained.

Keywords: Heat transfer in fluidized beds, second law efficiency, entropy generation, irreversibility, heat exchangers

1. Introduction

It is necessary to transfer a certain amount of heat to the coolant media in order to maintain the combustion temperature at an optimum level in a circulating fluidized bed (CFB) combustor. The studying of heat transfer from CFB combustor to the heat transfer surfaces in circulating fluidized beds is thus essential since most CFB applications, including combustion, calcination and hydrocarbon cracking, are operated at high temperatures. With better knowledge of heat transfer mechanisms, design and operation can be improved, and the energy evolved during the combustion process can be used with higher efficiency.

Numerous experimental and theoretical investigations to describe the heat transfer to the walls of fluidized beds have been studied since 1949 with the work of Mickley and Fairbanks (1955). Since then much experimental and modeling work has been done in both laboratory and industrial scale units. Leckner et al. (1991) identified two kinds of heat transfer processes in a CFB: thermal radiation and convection heat transfer between the particle-gas and the wall. The convection provides a larger proportion of the overall heat transfer (Gloriz, 1995). Subbarao and Basu (1986) used theoretical results in a bubbling fluidized bed to determine the area

averaged wall-clusters heat transfer coefficient and the area averaged wall-gas heat transfer coefficient. Yates (1996), Basu and Nag (1996) and Glicksman (1997) presented comprehensive reviews of CFB heat transfer. Recently, Pagliuso et al. (2000) experimentally investigated the local convection heat transfer coefficient. Grace et al. (2002) experimentally and theoretically investigated the effects of various operating parameters on the heat transfer process. Tian and Peng (2004) theoretically studied the particle-gas convection heat transfer coefficient. There have also been many studies concerning the fundamental analysis of the heat transfer between the fluidized beds and their immersed surfaces (Grace et al., 2000; Al-Busoul et al., 2000). Finned heat transfer studies in a CFB have also been reported in the literature (Basu et al., 1991; Nag and Moral, 1993; Reddy and Nag, 1997). Basu et al. (1991) made an experimental investigation to study the effect of fins on heat absorption in a cold CFB, under different operating conditions. Nag and Moral (1993) reported heat transfer results for pin-fins in a cold CFB. Reddy and Nag (1997) reported that short extended fins may be more effective in increasing the heat flow rate from the bed to the water wall tubes, and as for the extended fin, the fin efficiency decreases with an increase in fin length. Although there have been many studies

*Author to whom correspondence should be addressed

concerning the fundamental analysis of the heat transfer between the fluidized beds and their immersed surfaces as mentioned above, the second law analysis of the heat transfer to the combustor efficiency is very rare in the literature.

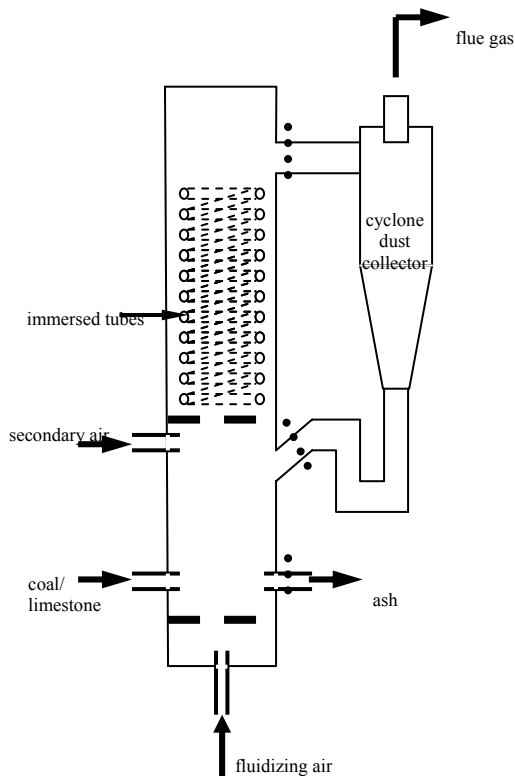


Figure 1. The scheme of the CFB combustor.

It is known that the heat input is proportional to the bed cross-section, whereas the heat absorption is proportional to the perimeter of the furnace. The cooling surfaces can either be vertical membrane walls, internal tubes (immersed surfaces) in the combustion chamber or tube bundles in an external heat exchanger in the particle recirculation loop. This study deals with heat transfer to the internal tubes with or without fins in laboratory scale fluidized beds, because immersed heat transfer surfaces are positively not used in large scale CFB boilers due to the erosion potential of the circulating bed medium. Larger furnaces and cooled cyclones are used instead, and in very large units, divided chambers and inner separators, to gain surface and achieve compactness. External tube bundles are always needed for economizers and steam heaters, and sometimes, at medium sizes, as additional evaporating loops.

The objectives of this study are to investigate the importance and extent of heat transfer surfaces in small-scale high temperature circulating fluidized beds through the second law of thermodynamics. A CFB combustor model is used to show how the immersed surfaces affect the thermodynamic efficiency of the combustor. The scheme of the combustor used in the analysis

is shown in *Figure 1*. Using the developed fluidized bed model of Eskin and Gungor (2001, 2003), the heat transfer coefficient in the CFB combustor has been calculated and the results are validated by the experimental data in the literature (Al-Busoul et al., 2000; Wunder, 1980). With these values, and using the developed simulation programs for bubbling and circulating fluidized bed combustors, the entropy generation rate and the second law efficiency of the combustors have been calculated and analyzed under different operating conditions considering the effectiveness of types of immersed surfaces.

2. System Analysis

In order to analyze the effect of the heat transfer surfaces on combustor efficiency, a CFB combustor model, which can be employed to simulate a wide range of operating conditions, was developed. The model includes volatilization, attrition and combustion of a char particle, respectively. In the modeling, the combustor riser is analyzed in two regions: a bottom zone considering a bubbling fluidized bed and an upper zone considering dilute phase and dense phase. In the bottom zone, a single-phase back-flow cell model is used to represent the solid mixing in the bed. The exchange of solids between the bubble phase and emulsion phase is a function of the bubble diameter and varies along the axis of the combustor. In the upper zone, core annulus flow structure is established based on the studies of previous researchers (Wang et al., 1999; Ryabov et al., 1999). Particles move upward in the core and downward in the annulus. The thickness of the annulus varies according to the combustor height. The structure and details of the model have been given in previous studies (Eskin and Gungor, 2001, 2003).

Based on the special hydrodynamics of the CFB combustor, the cluster renewal model of the bed to the immersed surface heat transfer process has been described in the literature (Wang et al., 1999; Ryabov et al., 1999). The dilute phase is comprised of a continuous upflowing gas phase with thinly dispersed solids and a relatively denser phase moving downward along the immersed heat transfer surfaces. Any part of the heat exchanger comes in alternative contact with the cluster and the dilute phase. If ε_c is the average fraction of the wall area covered by the clusters, the time-averaged total heat transfer coefficient, h_t , may be written as the sum of the convective and radiative heat transfer coefficients:

$$h_t = \varepsilon_c h_c + (1 - \varepsilon_c) h_d + \varepsilon_c h_{rc} + (1 - \varepsilon_c) h_{rd} \quad (1)$$

where h_c and h_d are the convective heat transfer coefficient for the cluster and the dispersed phase,

respectively (Wang et al., 1999; Ryabov et al., 1999; Wen and Miller, 1961; Basu et al., 1996).

$$h_c = \frac{k_g}{d} 0.009 \times \text{Pr}^{0.33} \text{Ar}^{0.5} \quad (2)$$

where Pr is the Prandtl number and Ar is the Archimedes number (Basu et al., 1996). The convection heat transfer from the dispersed phase to the wall is estimated by the modified equation of Wen and Miller (1961), which was given by Basu et al. (1996) as:

$$h_d = \left(\frac{k_g}{d_p} \right) \left(\frac{c_p}{c_g} \right) \left(\frac{\rho_d}{\rho_p} \right)^{0.3} \times \left(\frac{U_t^2}{g d_p} \right)^{0.21} \text{Pr} \quad (3)$$

The density of the dispersed phase ρ_d is given by:

$$\rho_d = \rho_p \varepsilon_p + \rho_g (1 - \varepsilon_p) \quad (4)$$

where ε_p is the volumetric concentration of particles in the dispersed phase.

At bed temperatures higher than 800° C, the available information suggests that the effect of radiation becomes significant. The cluster radiation component of the heat transfer coefficient is estimated from the following equation:

$$h_{rc} = \frac{s(T_p^4 - T_{he}^4)}{\left\{ (e_c^{-1} - e_b^{-1}) - 1 \right\} (T_p - T_{he})} \quad (5)$$

where e_c is the emissivity of the cluster and e_b is the emissivity of the immersed surfaces (Basu et al., 1996). For gray particles, it is fairly accurate to estimate the cluster emissivity from the particle emissivity (Grace et al., 2002).

$$e_c = 0.5(1 + e_p) \quad (6)$$

The dispersed phase radiation heat transfer coefficient from bed to immersed surfaces is estimated from the following equation (Basu et al., 1996):

$$h_{rd} = \frac{\sigma (T_b^4 - T_{he}^4)}{\left\{ (e_d^{-1} - e_b^{-1}) - 1 \right\} (T_b - T_{he})} \quad (7)$$

where e_d is the emissivity of the dispersed phase. For a very dilute medium, the effect of gas radiation can be taken into account as follows (Basu et al., 1996):

$$e_d = (e_g + e'_p - e_g e'_p) \quad (8)$$

The combustor has two main sections, bottom zone and upper zone, and in each zone it is divided into two phases: the dense phase and the dilute phase. According to the model, the fluidized bed is split up horizontally into individual cells in which the temperature and concentration within each cell is homogenous. Mass and energy balance equations at each cell are written separately for the volatile gases, oxygen, carbon monoxide, carbon dioxide, sulfur dioxide, nitric oxide and water vapor for each phase. The balance equations for the bed material, char, combustion gas components and energy for each cell are developed. The mass flow rate throughout the compartment can be expressed in terms of substances entering and leaving the compartment, \dot{m}_{in} and \dot{m}_{out} , as follows:

$$\dot{m}_{in,i-1} - \dot{m}_{out,i} = \frac{dm_i}{dt} \quad (9)$$

The char mass flow rate, \dot{m}_C throughout the compartment can be expressed as:

$$\dot{m}_{C,in,i-1} - \dot{m}_{C,out,i} - \Delta \dot{m}_{C,i} = \frac{d(m_{C,i})}{dt} \quad (10)$$

The energy balance equation in the i^{th} compartment can be expressed in terms of rate of change of energy as:

$$\dot{m}_{in,i-1} h_{in,i-1} - \dot{m}_{out,i} h_{out,i} + \dot{Q}_{release,i} - \dot{Q}_{w,i} - \dot{Q}_{wall,i} = \frac{d(m_i H_i)}{dt} \quad (11)$$

where $\dot{Q}_{w,i}$, the amount of heat transferred to the heat exchanger surfaces, is:

$$\dot{Q}_{w,i} = U_{he,i} A_{he,i} \Delta T_{m,i} \quad (12)$$

The finned surface heat transfer calculations take into account the fin efficiency and the surface area of the fin in the model simulation. The energy balance of the control volume used in the model for immersed surfaces is shown in Figure 2.

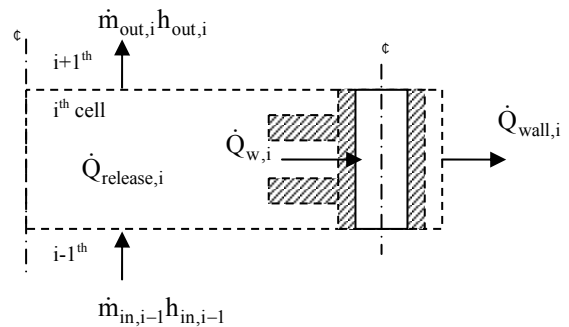


Figure 2. The energy balance of the control volume for immersed surfaces.

The Gouy-Stodola theorem states that the lost available work is directly proportional to the entropy generation in a non-equilibrium phenomenon of exchange of energy and momentum within the fluid and at the solid boundaries. For the purpose of evaluating the degree of irreversibility of the combustor, the entropy generation expression for each cell is obtained.

$$\begin{aligned} \dot{S}_{gen,t} = & \dot{S}_{gen(chem. react.)} \\ & + \dot{S}_{gen(heat trans.)} + \dot{S}_{gen(fluid fric.)} \end{aligned} \quad (13)$$

Here the first term on the right-hand side shows the entropy generated due to chemical reaction, while the entropy generated due to heat transfer, is shown by the second term. The third term is the entropy generation due to fluid friction in the combustor.

Recently, the irreversibility distribution parameter in the literature has been expressed by (Bejan, 1996).

$$\text{Bejan Number} = \frac{\dot{S}_{gen,heat transfer}}{\dot{S}_{gen,t}} \quad (14)$$

As the Bejan number gets closer to one, the irreversibility due to heat transfer dominates, whereas for the Bejan number near to zero, the irreversibility due to chemical reaction is more important.

The rate of entropy generation over the bed cross-section \dot{S}_{gen} can be calculated by integration:

$$\dot{S}_{gen} = \int_0^R \dot{S}_{gen,t,i} 2\pi r dr \quad (15)$$

Since the model provides a way to calculate the local velocity, temperature and concentration distributions within the compartment for each phase, a detailed calculation of the available energy loss, for various cooling tube arrangements, is possible. Therefore, for each compartment, the second law efficiency is calculated in terms of available energies as:

$$\eta_{II} = 1 - \frac{\chi_L}{\chi_{in}} \quad (16)$$

Here the lost available energy, which is the result of the irreversibilities in the compartment, is expressed in terms of substances entering and leaving the compartment \dot{m}_n and \dot{m}_k as follows;

$$\begin{aligned} \chi_L = & \sum_n \dot{m}_{n,i} a_n - \sum_k \dot{m}_{k,i} a_k \\ & + \dot{Q}_i \left(1 - \frac{T_0}{T} \right) \end{aligned} \quad (17)$$

3. Simulation Results and Discussion

To test and validate the formulation presented in this paper, the heat transfer coefficient was simulated for two different fluidized bed combustors, and the simulation results are compared with the experimental results of different researchers (Al-Busoul et al., 2000; Wunder, 1980; Wang et al., 1999).

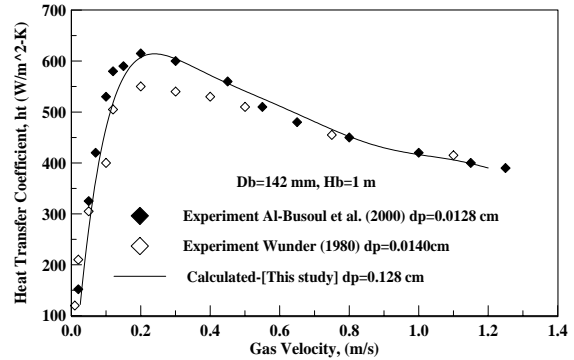


Figure 3. Heat transfer coefficient as a function of gas velocity for various diameters of solid particles: Comparison of simulation results with experimental data.

The heat transfer model takes into consideration the parameters, which are relevant to heat transfer in a fluidized bed. In these comparisons, total and convective heat transfer coefficients along the bed height are obtained for a 12 MW CFB combustor unit (Wang et al., 1999) and the total heat transfer coefficient as a function of gas velocity obtained from the experiments of two different researchers (Al-Busoul et al., 2000; Wunder, 1980) using the same input variables in the experiments as the simulation program input.

The results obtained from the model for particle size 0.128 cm and those from the experiments of different researchers (Al-Busoul et al., 2000; Wunder, 1980) are shown in Figure 3 as a function of gas velocity. The experiments were performed with an atmospheric fluidized bed in which air velocities were varied from 0.02 to 1.5 m/s. In these experiments, the test units were 1m high and the main column diameter was 142 mm. This figure shows a sharp rise in the heat transfer coefficient as velocity increases, until a maximum value is reached at a velocity 3 to 4 times the minimum fluidizing velocity (U_{mf}). This is due to the good mixing of bed material as the bed operational velocity increases. At higher gas velocities, a fall in the heat transfer coefficient occurred which persisted with a further increase in velocity. As the velocity increased to a value greater than four times U_{mf} , the fluidized bed expanded to a very large extent, and the solid particles swept the heat exchanger

section faster, resulting in a reduced heat transfer coefficient. *Figure 3* demonstrates a very reasonable agreement with the predicted values of both experimental data. This agreement, over a wide range of fluidizing conditions, shows the applicability of the heat transfer model to small-size fluidized beds.

Figure 4 shows a comparison between the predicted total and the convective heat transfer coefficients with the experimental results obtained for a 12 MW CFB combustor (Wang et al., 1999).

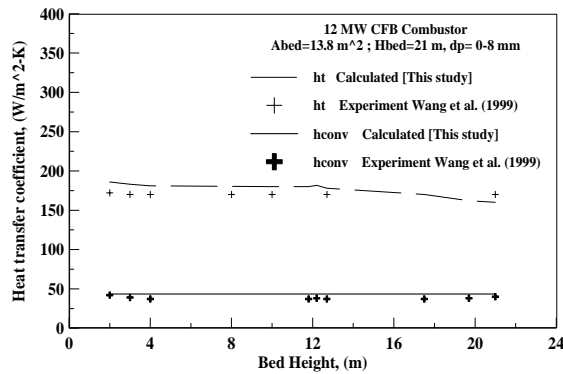
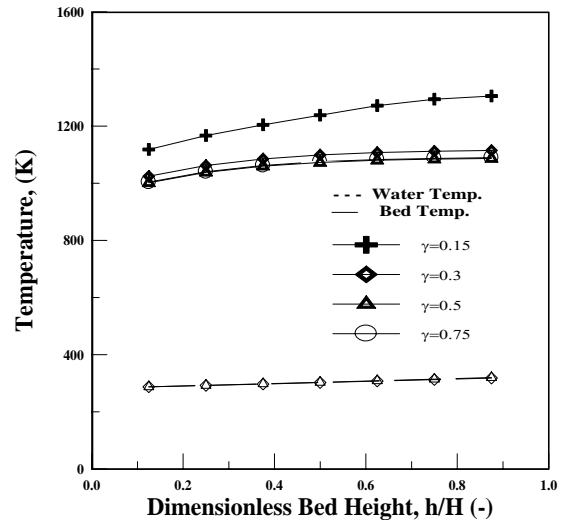


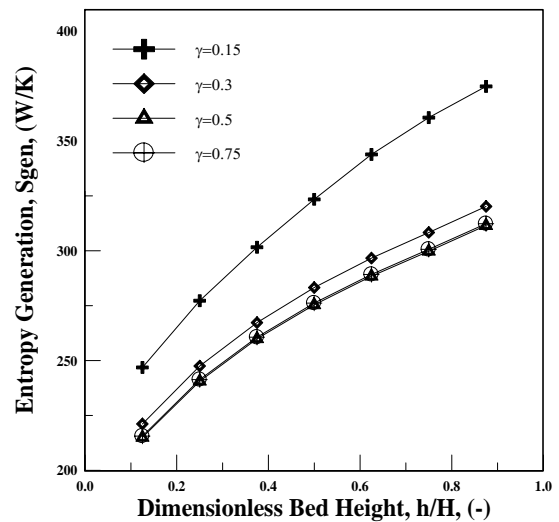
Figure 4. Variation of heat transfer coefficients in the combustor.

The test rig was a bituminous-fired combustor with 21m height and 4.2 m diameter. Whereas the predicted convective heat transfer coefficient values are in agreement with the experimental ones (maximum 1.8%), there is some deviation (maximum 4.7%) in total heat transfer coefficient values. This difference is due to the uncertainties in the measurements, which were given as 1.2% (Wang et al., 1999), and due to predicted particle temperatures used in the radiative heat transfer coefficient calculation. Simulation results agree with the experimental results and show the applicability of the heat transfer model to the CFB combustors.

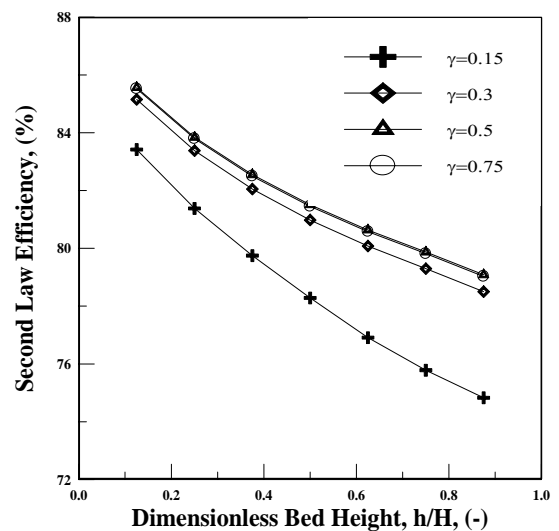
Using the heat transfer model, the second law efficiency of the CFB combustor was obtained. In performing the simulations, the volume ratio, γ , which is the ratio of the volume of heat transfer surfaces to the combustor volume, was defined. The effect of immersed heat transfer surfaces on CFB combustor efficiency along the bed height is shown in *Figure 5*. Efficiency decreases with bed height at each γ value, and its value at every level in the furnace increases as the value of γ increases up to $\gamma=0.50$. The slope of decrease, especially at lower γ values, is bigger due to the variation in temperature distribution within the combustor. At a higher volume ratio, the combustor efficiency value stays constant due to the moderate combustor temperatures.



(a)



(b)



(c)

Figure 5. Variation of bed temperature (a), entropy generation (b), and second law efficiency (c) along the bed height.

The model results are obtained for different types of fluidizing bed combustors which have the same dimensions of 20 cm i.d. and 110 cm height. Coal particles with a mean size of 1.5 mm and particle density 1.4 kg/m³ are considered for model calculations. The variation of second law efficiency with bed velocity ratio is presented in *Figure 6* for two different types of fluidized bed (circulating (CFB) and bubbling (BFB)) combustors. As can be observed, both combustor efficiencies increase with increasing γ values. Both BFB and CFB combustor efficiencies decrease with increasing gas velocities at a faster rate, indicating that the higher gas velocities affect bed hydrodynamics and decrease the heat transfer coefficient, which in turn affects the heat transfer rate at each γ value.

BFB combustor efficiencies at the same velocity ratio are lower than CFB combustor efficiencies at constant heat exchanger volume ratios. This is due to the high amount of the solid entrainment rate from the bed section and low heat transfer coefficients at high gas velocities.

The influence of heat exchanger types on entropy generation and combustor efficiency for two different types of combustors (CFB and BFB combustors) is compared in *Figure 7* and *Figure 8*, respectively.

In order to compare the influence of the heat exchanger type on the combustor efficiency, these profiles are obtained for different types of heat exchangers - immersed tubes, immersed tubes with lateral and extended fins at different fin lengths. Fin lengths have been changed between 1 mm and 15 mm with a 1 mm interval. It is estimated from the simulation results that up to a 5 mm fin length, the combustor efficiency, remains more or less the same. Afterwards it starts decreasing at a faster rate, indicating that the short extended fins are more effective in absorbing heat from the bed. In the figures, two fin lengths, 5 mm and 10 mm, are presented.

Using the heat exchanger surfaces with extended fins in fluidized bed combustors, entropy generation due to chemical reactions and fluid friction are the dominant factors as operating velocity increases. Using the extended fins heat exchanger in CFB is more effective than in BFB under the same operating conditions. The short fins do not affect much of the bed hydrodynamics, which in turn result in less entropy generation than the longer ones. Thus small-extended fins both in BFB and CFB combustors may be preferred since they increase heat absorption as observed in the present investigation.

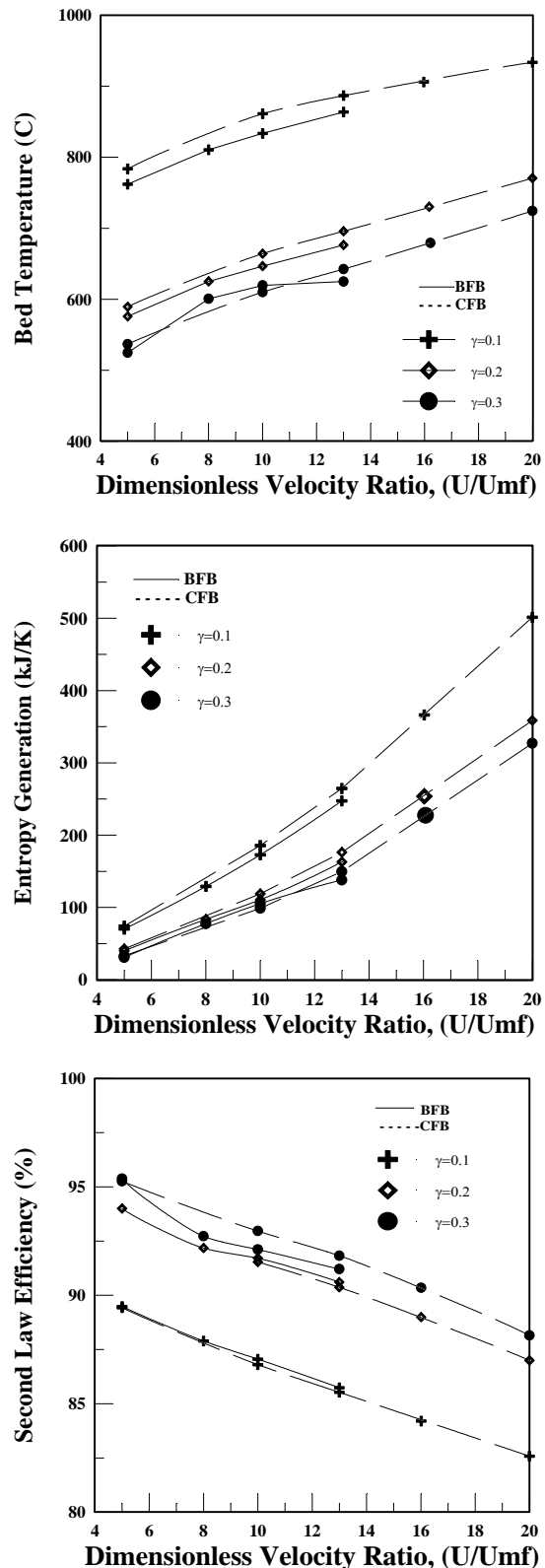


Figure 6. Variation of bed temperature, entropy generation and second law efficiency for immersed tubes.

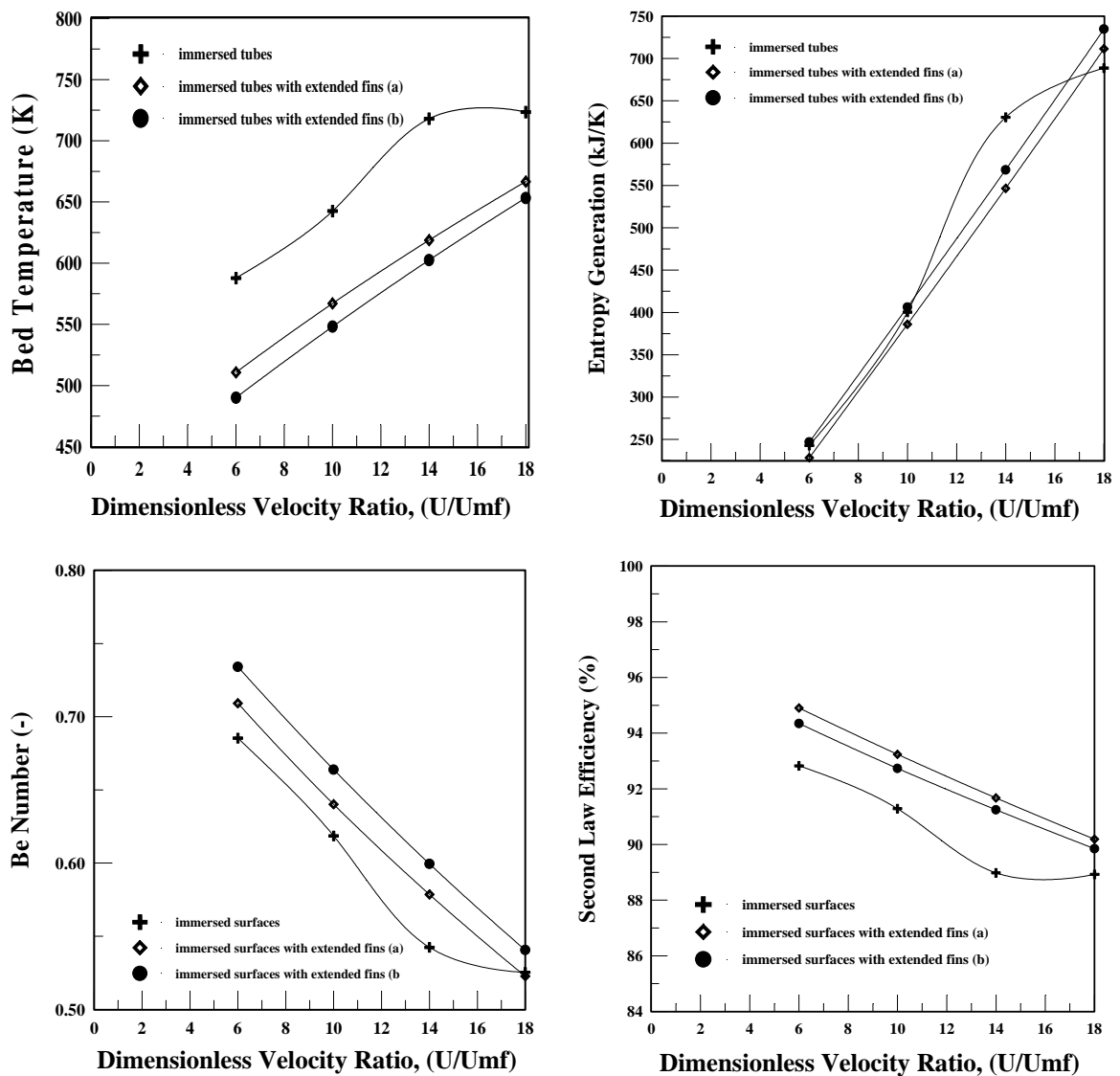


Figure 7. Comparison of bed temperature, Bejan number, entropy generation, and second law efficiency of heat exchanger surfaces for BFB: (a) = 5 mm fin length, (b) = 10 mm fin length.

4. Conclusions

The thermodynamic analysis of heat transfer to the immersed surfaces in small-scale circulating fluidized beds is very important to show how the parameters affect the efficiency of a fluidized bed combustor. Combustor efficiency was examined under various conditions and for different types of heat exchanger surfaces. It decreases along the bed height at each γ - volume ratio. On the other hand, efficiency at every level in the combustor increases as the value of γ increases, up to 0.5. At higher volume ratios, the combustor efficiency value stays almost constant due to the moderate combustor temperatures.

Both for circulating fluidized bed combustors and for bubbling bed combustors, for a given velocity ratio, combustor efficiency

increases as γ - heat exchanger volume ratio increases. This ratio is more dominant in combustor efficiency in circulating fluidized bed combustors.

In this simulation, the type of heat exchanger surfaces is also considered. Using the heat exchanger surfaces with extended fins in fluidized bed combustors, entropy generation due to chemical reactions and fluid friction is the dominant factor as operating velocity increases. The short fins do not affect much of bed hydrodynamics, which in turn results in less entropy generation than the longer ones. Thus small-extended fins both in BFB and CFB combustors may be preferred because they increase combustor efficiency, as observed in the present investigation.

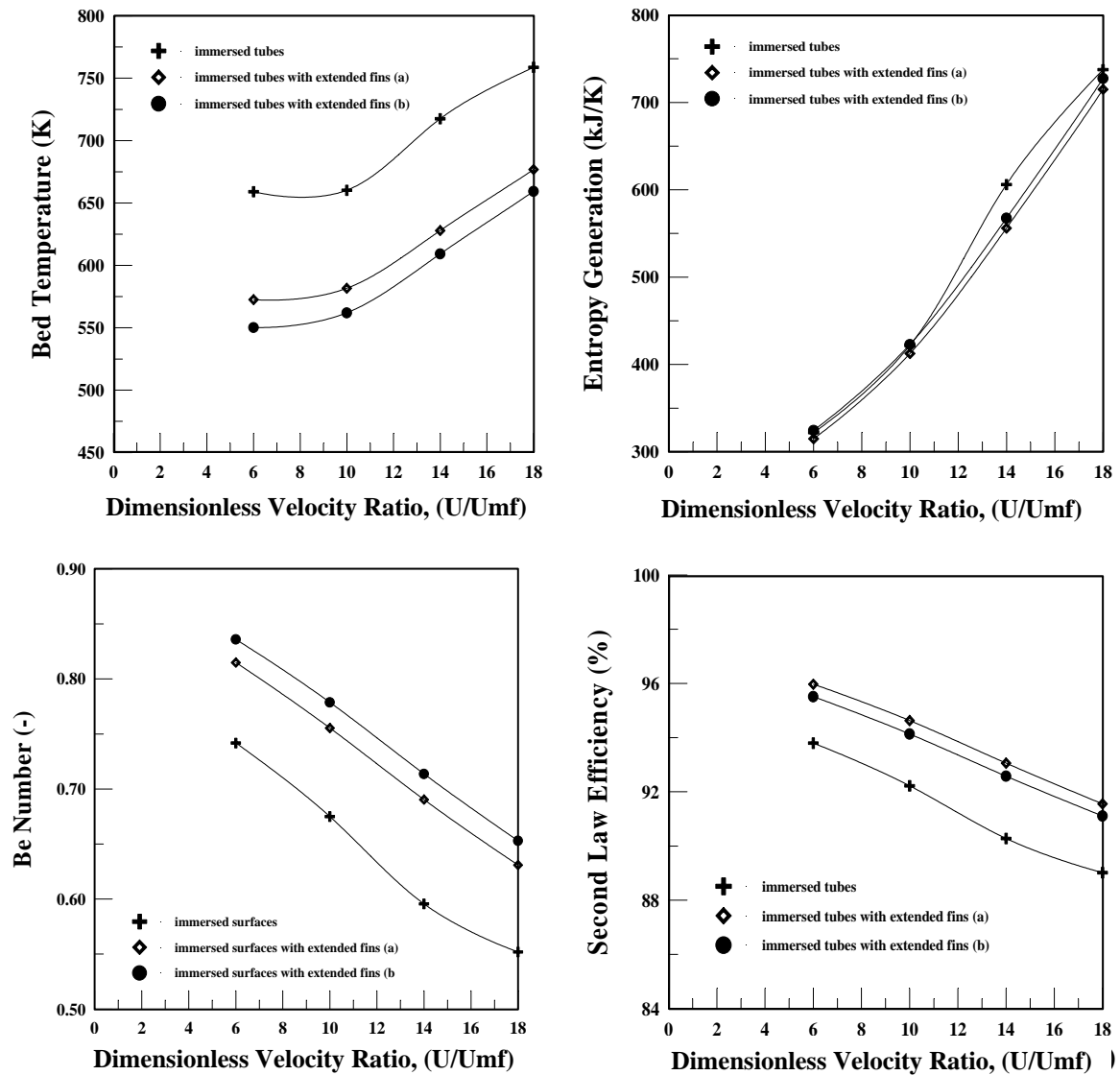


Figure 8. Comparison of bed temperature, Bejan number, entropy generation, and second law efficiency of heat exchanger surfaces for CFB: (a) = 5 mm fin length, (b) = 10 mm fin length.

Nomenclature

A	Area [m ²]	h_{rc}	Radiative heat transfer coefficient for clusters [W/m ² K]
a	Availability [kJ/kg]	h_{rd}	Radiative heat transfer coefficient for dispersed phase [W/m ² K]
c	Specific heat capacity [kJ/kgK]	h_t	Total heat transfer coefficient at combustor side [W/m ² K]
D	Diameter [m]	k_g	Gas conduction heat transfer coefficient [W/m K]
d_p	Particle diameter [m]	m	Mass [kg]
\bar{d}	Mean diameter [m]	\dot{m}	Mass flow rate [kg/s]
e	Emissivity [-]	\dot{Q}	Amount of heat transferred [kW]
e'_p	Effective emissivity of particle cloud [-]	\dot{S}_{gen}	Entropy generation [kW/K]
H	Enthalpy [kJ/kg]	T	Temperature [K]
H_b	Bed height [m]	t	Time [s]
h	Heat transfer coefficient [W/m ² K]; compartment height [m]	U	Overall heat transfer coefficient [kW/m ² K]
h_c	Convection heat transfer coefficient for clusters [W/m ² K]	U_t	Particle terminal velocity [m/s]
h_d	Convection heat transfer coefficient for dispersed phase [W/m ² K]		

Greek Symbols

$\Delta\dot{m}_{C,i}$	Carbon mass flow rate consumed from physical and chemical processes [kg/s]
ΔT_m	Log-mean temperature difference [°C]
ε	Void Fraction [-]
ε_c	Averaged fraction of wall area covered by clusters [-]
ε_p	Volumetric concentration of particles in the dispersed phase [-]
ρ	Density [kg/m ³]
γ	Volume ratio [-]
σ	Stefan-Boltzman constant [W/m ² K ⁴]
η_{II}	Second law efficiency [-]
χ	Available energy, exergy [kW]

Subscripts

b	Bed
C	Carbon
c	Cluster
d	Dispersed
g	Gas
he	Immersed surfaces
i	Compartment number
in	Input
L	Lost
o	Reference
out	Output
p	Particle
t	Total
w	Water
wall	Wall

References

- Al-Busoul, M., Abu-Zahid, M., 2000, "Prediction of Heat Transfer Coefficient Between Immersed Surfaces and Fluidized Beds", *Int. Com. Heat Mass Transfer*, Vol. 27, No. 4, pp. 549-558.
- Basu, P., Moral A. M. N. and Nag, P. K., 1991, "An Experimental Investigation Into the Effect of Fins on Heat Transfer in Circulating Fluidized Beds", *Int.J. Heat Mass Transfer* Vol. 34, pp. 2317-2326.
- Basu, P., Cheng, L., Cen, K., 1996, "Heat Transfer in a Pressurized Circulating Fluidized Bed", *Int. J. Heat Mass Transfer*, Vol. 39, pp. 2711-2722.
- Basu, P., Nag, P. K., 1996, "Heat Transfer to Walls of a Circulating Fluidized-Bed Furnace", *Chemical Engineering Science*, Vol. 51, No. 1, pp.,1-26.
- Bejan, A., 1996, *Entropy Generation Minimization*. CRC Press, Boca Raton, New York, London, Tokyo.
- Eskin, N., Güngör, A., 2001, "Thermodynamic Analysis of Heat Transfer to the Immersed Surfaces in a Circulating Fluidized Bed",

Proceedings of ECOS 2001, Öztürk, A., Gögüş, Y. A., eds., İstanbul, Vol. 1, pp. 249-256.

Eskin, N., Güngör, A., 2003, "A Model for Circulating Fluidized Bed Combustors", *Proceedings of IEEEES-1*, Dinçer, İ., Hepbaşlı, A., eds., Izmir, pp. 911-918.

Glicksman, L. R., 1997, "Heat Transfer in Circulating Fluidized Beds", *Circulating Fluidized Beds*, Blackie Academic & Professional (Chapman and Hall), Grace, J. R., Avidan, A. A. & Knowlton, T. M. (eds.), London, pp. 261-311 (Chapter 8).

Gloriz, M. R., 1995, "An Experimental Correlation for Temperature Distribution at the Membrane Wall of CFB Boilers", *Proceedings of 13th International Conference on Fluidized Bed Combustion*, Orlando; pp. 167-174.

Grace, J. R., Luan, W., Bowen, B. D., Lim, C. J., Brereton, C. M. H., 2000, "Suspension-to-Membrane-Wall Heat Transfer in a Circulating Fluidized Bed Combustor", *Int.J. Heat Mass Transfer*, Vol. 43, pp. 1173-1185.

Grace, J. R., Xie, D., Bowen, B. D., Lim, C. J., 2002, "Two-Dimensional Model of Heat Transfer in Circulating Fluidized Beds. Part II: Heat Transfer in a High Density CFB and Sensitivity Analysis", *Int.J. Heat Mass Transfer*, Vol. 46, pp. 2193-2205.

Leckner, B., Gloriz, M. R., Zhang, W., Anderson, B. A., 1991, "Boundary Layer-First Measurement in the 12 MW Research Plant at Chalmers University", *Proceedings of the 1991 International Conference on Fluidized Bed Combustion*, Anthony E. J., ed., Montreal, pp. 771-776.

Mickley, H. and Fairbanks, D., 1955, "Mechanism of Heat Transfer to Fluidized Beds", *A.I.Ch.E.J.* Vol 1, pp. 374-384.

Nag, P. K. and Moral A. M. N., 1993, "An Experimental Study of the Effect of Pin-Fins on Heat Transfer in Circulating Fluidized Beds", *Int. J. Energy Research*, Vol. 17, pp. 863-872.

Pagliuso J. D., Lombarbi G., Goldstein J. L., 2000, "Experiments on the Local Heat Transfer Characteristics of a Circulating Fluidized Bed", *Experimental Thermal and Fluid Science*, Vol.20, No.3-4, pp.170-179.

Reddy, B. V. and Nag, P. K., 1997, "Effect of Lateral and Extended Fins on Heat Transfer in a Circulating Fluidized Bed", *Int.J. Heat Mass Transfer*, Vol. 41, No. 1, pp. 139-146.

Ryabov, G. A., Kuruchkin, A. I., Folomeev, O. M., 1999, "Investigation of Heat Transfer to the Waterwalls on an Aerodynamic Model of a Circulating Fluidized-Bed Boiler", *Thermal Engineering*, Vol. 46, No. 8, pp. 674-680.

Subbarao, D., Basu, P., 1986, "Heat Transfer in Circulating Fluidized Beds", *Circulating Fluidized Bed Technology*, Basu P., ed., Pergamon Press, Oxford.

Tian, Y. and Peng, X. F., 2004, "Analysis of Particle Motion and Heat Transfer in Circulating Fluidized Beds", *Int.J. Energy Research*, Vol. 28, pp. 287-297.

Wang, Q., Luo, Z., Li, X., Fang, M., Ni, M., Cen, K., 1999, "A Mathematical Model for a Circulating Fluidized Bed (CFB) Boiler", *Energy*, Vol. 24, pp. 633-653.

Wen, C. Y., Miller, E. N., 1961, "Heat Transfer in Solid-Gas Transport Lines", *Industrial Eng. Chem.*, Vol. 53, pp. 51-53.

Wunder, R., 1980, "Heat Transfer Analysis in Fluidized Beds", Ph.D. dissertation, Tu Munchen.

Yates, J. G., 1996, "Effects of temperature and pressure on gas-solid fluidization", *Chemical Engineering Science*, Vol. 51, No. 2, pp.167-205.